DALTON

Dimer species in dimethyl sulfoxide–water (80:20 w/w) solution of *N*,*N*′-bis(salicylideneimine)-*m*-phenylenediamine (H_2sal-*m*-phen) and similar Schiff bases with Cu^{II}, Ni^{II}, Co^{II} and Zn^{II}. Crystal structure of $[Co_2(sal\text{-}m\text{-}phen)_2]\cdot CHCl_3$ ‡

Rita Hernández-Molina,[a] Alfredo Mederos,*,†,[a] Pedro Gili,[a] Sixto Domínguez,[a] Francesc Lloret,[b] Joan Cano,[b] Miguel Julve,[b] Catalina Ruiz-Pérez[c] and Xavier Solans[d]

[a] *Departamento de Química Inorgánica, Universidad de La Laguna, 38200 La Laguna, Tenerife, Canary Islands, Spain*
[b] *Departament de Química Inorgànica, Universitat de València, Dr. Moliner 50, 46100 Burjassot (València), Spain*
[c] *Departamento de Física Fundamental y Experimental, Universidad de La Laguna, 38200 La Laguna, Tenerife, Canary Islands, Spain*
[d] *Departament Cristal.lografia, Mineralogia i Dipòsits Minerals, Universitat de Barcelona, Martí i Franqués s/n, 08028 Barcelona, Spain*

Potentiometric studies were carried out in dimethyl sulfoxide–water (80:20 w/w) at 25 °C and ionic strength 0.1 mol dm^{-3} in $NaClO_4$ for the Schiff bases H_2sal-*m*-phen [*N*,*N*′-bis(salicylidene)-*m*-phenylenediamine], H_2sal-2,4-toluen [*N*,*N*′-bis(salicylidene)toluene-2,4-diamine] and H_2sal-2,6-toluen [*N*,*N*′-bis(salicylidene)toluene-2,6-diamine] and their complexes with Cu^{II}, Ni^{II}, Co^{II} and Zn^{II}. These studies have shown that monomer, dimer, ligand:metal ratio 2:1 and 1:2 complex species are found. The first reported stability constants for these systems have been determined. The molecular structure of the complex $[Co_2(sal\text{-}m\text{-}phen)_2]\cdot CHCl_3$ has been determined by single-crystal X-ray analysis. It consists of dimeric centrosymmetric units, with the two bis(salicylideneiminato)-cobalt(II) residues bridged by two *m*-phenylene groups and with a chloroform molecule associated with each dimer molecule. The co-ordination geometry around each cobalt(II) can be best described as a distorted tetrahedron. Variable-temperature magnetic susceptibility measurements for the solid complexes $[Co_2(sal\text{-}m\text{-}phen)_2]\cdot CHCl_3$, $[Co_2(sal\text{-}2,4\text{-}toluen)_2]\cdot 4H_2O$, $[Co_2(sal\text{-}2,6\text{-}toluen)_2]$, $[Ni_2(sal\text{-}m\text{-}phen)_2]\cdot 3H_2O$, $[Ni_2(sal\text{-}2,4\text{-}toluen)_2]\cdot 3H_2O$, $[Ni_2(sal\text{-}2,6\text{-}toluen)_2]$, $[Cu_2(sal\text{-}2,4\text{-}toluen)_2]$ and $[Cu_2(sal\text{-}2,6\text{-}toluen)_2]$ revealed a weak intradimer antiferromagnetic interaction.

The preparation of co-ordinating agents derived from aromatic diamines is of special interest since the use of nitrogen atoms for co-ordination of a single cation is directly related to their relative *ortho*, *meta* or *para* positions, as shown for tetramethylcarboxylic acids.[1–11] Thus, for Schiff bases derived from *o*-phenylenediamines, the proximity of the nitrogen atoms permits simultaneous co-ordination of both to the same metal cation, as has been established by the X-ray crystallographic determination of the structure of the complexes of *N*,*N*′-bis(salicylidene)-*o*-phenylenediamine (H_2sal-*o*-phen) with Co^{II} [12] and *N*,*N*′-bis(salicylidene)toluene-3,4-diamine (H_2sal-3,4-toluen) with Ni^{II}.[13] These Schiff bases are tetradentate and form complexes basically with a square-planar geometry with these metals. On the other hand, Schiff bases derived from *m*-phenylenediamines (Scheme 1) can only co-ordinate one nitrogen atom to any metal cation,[7–9] facilitating the formation of dimer complexes, where the ligands act as a bridge between both metal cations. This has been proven by means of X-ray diffraction analyses for a complex of sal-*m*-phen with Cu^{II},[14] and by mass spectrometry of the dimeric complexes of Cu^{II} and Co^{II} with *N*,*N*′-bis(1-acetylprop-2-ylidene)-*m*-phenylenediamine (H_2acac-*m*-phen).[15]

Thermodynamic data for Schiff-base complexes derived from diamines and aldehydes are in general scarce, due mainly to the insolubility in water of such compounds. The few previously reported stability constants are related to Schiff bases derived from *o*-phenylenediamines or ethane-1,2-diamines with salicylaldehyde.[13,16–20] For complexes derived from *m*-phenylenediamines all the research has been restricted to their synthesis

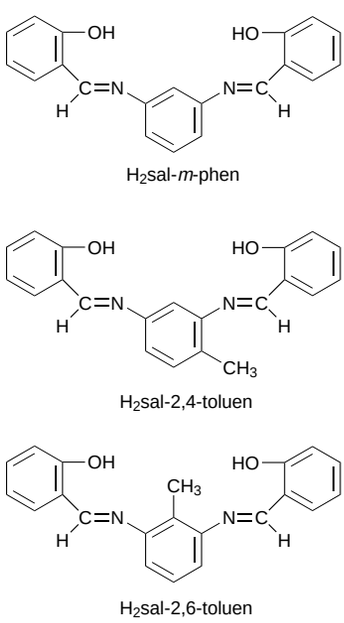

Scheme 1

† E-Mail: amederos@ull.es
‡ *Supplementary data available* (No. SUP 57286, 10 pp.): species distributions, stability constants. See *J. Chem. Soc.*, *Dalton Trans.*, 1997, Issue 1.

and structural characterization.[14,15,21] However, their behaviour in solution has not been studied yet.

In this work we have determined by potentiometry the first reported stability constants of the systems H_2sal-*m*-phen, H_2sal-2,4-toluen and H_2sal-2,6-toluen with Cu^{II}, Ni^{II}, Co^{II} and Zn^{II}, in dimethyl sulfoxide–water (80:20 w/w) at 25 °C and $I = 0.1$ mol dm^{-3} $NaClO_4$. We also report on the crystal structure for $[Co_2(sal\text{-}m\text{-}phen)_2]\cdot CHCl_3$ and the magnetic properties of the copper(II), nickel(II) and cobalt(II) complexes.

Experimental

Materials

The Schiff-base ligands sal-*m*-phen, sal-2,4- and sal-2,6-toluen were synthesized by condensing the corresponding diamines with salicylaldehyde (ratio 1:2) in ethanol as reported previously.[21] Cobalt(II) acetate tetrahydrate, copper(II) acetate hexahydrate and nickel(II) acetate tetrahydrate from Merck were used without further purification. Dimethyl sulfoxide (dmso) (Merck p.a.) was purified by distillation under reduced pressure (*ca.* 2 Torr; 1 Torr ≈ 133 Pa) and stored in a dark bottle over 4 Å molecular sieves. From this solvent the mixture dmso–water (80:20 w/w) was prepared. All the solutions used in the potentiometric studies were prepared with this mixed solvent. The stock metal solutions (in perchlorate form) were prepared from the Aldrich perchlorates and standardized by complexometric titrations according to the procedure of Schwarzenbach.[22] A carbonate-free sodium hydroxide solution prepared from an ampoule of 9959 Titrisol (Merck) and perchloric acid (Merck) solution were used as titrants in the potentiometric studies. Sodium perchlorate was prepared by recrystallization of the Merck product and then used as a background electrolyte.

Potentiometric measurements

The potentiometric technique is described in a previous paper.[23] The potentiometric studies were carried out in dmso–water (80:20 w/w) solution at ionic strength 0.1 mol dm^{-3} in $NaClO_4$ and 25 °C. The measurements were made using a Radiometer PHM-85 potentiometer and a Radiometer GK 2401 B combined electrode. The electrode was modified by replacing its aqueous KCl solution with a 0.5 mol dm^{-3} dmso–water (80:20 w/w) solution of $NaClO_4$. A BASIC program[24] (APT program for microcomputer ITS80286) was used to monitor the electromotive force values and the volume of titrant added for each titration point. The cell constants E° and the liquid-junction potentials J were measured according to the method of Biedermann and Sillen,[25] by means of a least-squares program before each experiment. The autodissociation constant of the solvent pK_w was 18.35, in good agreement with reported data.[17] This constant was determined at the beginning of each experiment to verify the correct working of the electrode and the reliability of the potential measurements.

Potentiomeric titrations of the Schiff bases were performed at the concentrations $c_L = (2.0–4.0) \times 10^{-3}$ mol dm^{-3} (titrations with NaOH and $HClO_4$) and in the presence of the metal at the metal:Schiff base ratios 2:1, 1:1 and 1:2 (titrations with NaOH). The metal concentration c_M was varied from 0.5×10^{-3} to 4.0×10^{-3} mol dm^{-3}. Concentrations higher than 4×10^{-3} mol dm^{-3} could not be investigated due to precipitation of the complexes.

The SUPERQUAD program[26] was used to process all the data and calculate both the protonation and stability constants.

Other physical measurements

Analyses (C, H, and N) were performed on a Carlo Erba 1106 automatic analyser. Infrared spectra were measured as KBr discs in the range 4000–250 cm^{-1} using a Nicolet 710 FT-IR spectrometer, electronic spectra in the solid state on a Beckman DU-2 spectrophotometer (sample dispersed in $BaSO_4$) and in solution on a Shimadzu UV-2101PC spectrophotometer and mass spectra by electron impact on a VG Micromass ZAB-2F instrument, the ionization voltage being 70 eV (*ca.* 1.12×10^{-17} J) and the temperature 473 K. Magnetic susceptibility measurements were carried out in the temperature range 4–300 K with a fully automatized AZTEC DSM8 pendulum-type susceptometer equipped with a TBT continuous-flow cryostat and a Bruker BE15 electromagnet operating at 1.8 T. The apparatus was calibrated with mercury tetra(thiocyanato)cobaltate(II). Diamagnetic corrections to the susceptibility of the complexes were calculated from Pascal's constants.[27]

Preparation of the complexes

The complexes $[Co_2(sal\text{-}m\text{-}phen)_2]\cdot CHCl_3$, $[Ni_2(sal\text{-}m\text{-}phen)_2]\cdot 3H_2O$, $[Ni_2(sal\text{-}2,4\text{-}toluen)]\cdot 3H_2O$, $[Co_2(sal\text{-}2,4\text{-}toluen)]\cdot 4H_2O$, $[Cu_2(sal\text{-}2,4\text{-}toluen)_2]$, $[Cu_2(sal\text{-}2,6\text{-}toluen)_2]$, $[Ni_2(sal\text{-}2,6\text{-}toluen)_2]$ and $[Co_2(sal\text{-}2,6\text{-}toluen)]$ were prepared in a similar way to the literature method.[28] The necessary basic medium for the formation of the dimer complexes was provided by the metal acetate used in the synthesis.

Red prismatic single crystals suitable for X-ray crystallography of $[Co_2(sal\text{-}m\text{-}phen)_2]\cdot CHCl_3$ were grown from a chloroform solution of the complex (Found: C, 57.09; H, 3.48; N, 6.48. Calc. for $C_{41}H_{29}Cl_3Co_2N_4O_4$: C, 56.83; H, 3.35; N, 6.46%). The most intense peaks in the mass spectrum were at *m*/*z* (relative intensity in %) 82 (100), 202 (45) and 244 (29); peaks of dimer, 424 (15), 449 (14), 579 (14), 614 (9), 723 (12) and 785 (7). The diffuse reflectance spectrum showed bands at 340 (broad; ligand-to-metal charge transfer, LMCT), 500–550 (sh) [$^4T(P) \longrightarrow {}^4A_2$] and 960 nm [$^4T_1(F) \longrightarrow {}^4A_2$];[29] free Schiff base[21] 460 nm ($n \longrightarrow \pi^*$). The UV–VIS spectrum in chloroform showed a band at 400 nm ($\varepsilon = 1.8 \times 10^4$ dm^3 mol^{-1} cm^{-1}) (LMCT).[29] Attempts to produce diffraction-quality crystals from the remaining complexes were unsuccessful.

$[Ni_2(sal\text{-}m\text{-}phen)_2]\cdot 3H_2O$ (Found: C, 59.33; H, 4.12; N, 6.37. Calc. for $C_{40}H_{36}N_4Ni_2O_4$: C, 59.89; H, 4.49; N, 6.99%): diffuse reflectance spectrum 400 (LMCT), 650 and 1000 nm (LFT).[29] $[Cu_2(sal\text{-}2,4\text{-}toluen)_2]$ (Found: C, 63.94; H, 4.09; N, 7.15. Calc. for $C_{42}H_{32}Cu_2N_4O_4$: C, 64.37; H, 4.09; N, 7.15%): mass spectrum *m*/*z* 68 (100), 185 (59), 225 (20), 312 (19) and 383 (7), peaks of dimer 447 (8) and 767 (21%); diffuse reflectance spectrum 540 nm (LMCT) and 700 nm (LFT).[29] $[Ni_2(sal\text{-}2,4\text{-}toluen)_2]\cdot 3H_2O$ (Found: C, 59.39; H, 4.36; N, 6.03. Calc. for $C_{42}H_{38}N_4Ni_2O_7$: C, 60.91; H, 4.59; N, 6.78%). $[Co_2(sal\text{-}2,4\text{-}toluen)_2]\cdot 4H_2O$ (Found: C, 59.01; H, 4.17; N, 6.10. Calc. for $C_{42}H_{40}Co_2N_4O_8$: C, 59.59; H, 4.73; N, 6.62%): mass spectrum *m*/*z* 69 (100), 129 (28), 185 (18), 236 (20), 353 (20) and 367 (24); peaks of dimer: 493 (11), 522 (10) and 578 (3%); diffuse reflectance spectrum 410 nm (LMCT), 582 (LFT) and 750 (br) (LFT).[29] $[Cu_2(sal\text{-}2,6\text{-}toluen)_2]$ (Found: C, 64.49; H, 4.20; N, 7.17. Calc. for $C_{42}H_{32}Cu_2N_4O_4$: C, 64.37; H, 4.08; N, 7.15%): mass spectrum *m*/*z* 69 (100), 121 (20), 132 (20), 145 (22), 183 (57), 225 (14) and 326 (9); peak of dimer 430 (15%); diffuse reflectance spectrum 380–410 (LMCT) and 760 nm (LFT).[29] $[Ni_2(sal\text{-}2,6\text{-}toluen)_2]$ (Found: C, 64.73; H, 4.29; N, 7.15. Calc. for $C_{42}H_{32}N_4Ni_2O_4$: C, 65.16; H, 4.14; N, 7.24%): mass spectrum *m*/*z* 69 (100), 145 (36), 183 (18) and 369 (4); peaks of dimer 430 (4) and 472 (7%); diffuse reflectance spectrum 400 (LMCT), 610 and 1050 nm (LFT).[29] $[Co_2(sal\text{-}2,6\text{-}toluen)_2]$ (Found: C, 64.23; H, 4.23; N, 7.11. Calc. for $C_{42}H_{32}Co_2N_4O_4$: C, 65.16; H, 4.14; N, 7.24%): mass spectrum *m*/*z* 69 (100), 145 (28), 183 (71) and 368 (4); peaks of dimer 446 (9) and 527 (4%); diffuse reflectance spectrum 350 and 540 nm; UV/VIS in chloroform 387 (ε *ca.* 1.8) and 348 nm (ε *ca.* 3.6×10^4 dm^3 mol^{-1} cm^{-1}) (LMCT).[29] Only the mass spectra of the dimer complexes that have been well resolved are included. IR spectra (cm^{-1}) ν(CN) 1606–1608 cm^{-1},[30–32] ν(CO) 1313–1328 cm^{-1} [31,32] for all

Table 1 Ionization constants (pK_i) of H_2sal-*m*-phen, H_2sal-2,4- and H_2sal-2,6-toluen in dmso–water (80:20 w/w) at 25 °C and $I = 0.1$ mol dm^{-3} $NaClO_4$

	pK_i			
Equilibrium	sal-*m*-phen	sal-2,4-toluen	sal-2,6-toluen	3-F-sal-*o*-phen[b]
L^{2-}/HL^-	10.49(1)[a]	10.61(1)	10.72(1)	11.23(2)
HL^-/H_2L	9.30(1)	9.43(1)	9.42(1)	8.41(5)
H_2L/H_3L^+	3.70(1)	3.96(1)	3.80(1)	3.17(4)
σ, χ^2	3.6, 4.3	2.9, 5.5	3.5, 12.8	
No. titrations	5	5	6	
No. points	132	230	199	
$-\log[H^+]$ range	2.5–10.5	2.5–10.3	2.3–10.3	

[a] Values in parentheses are standard deviations in the last significant digit. [b] Values in dioxane–water (70:30 v/v), $I = 0.1$ mol dm^{-3} in KCl taken from ref. 20.

complexes; ν(OH) 3400 cm^{-1} for complexes with water molecules.[28]

Crystallography

Crystal data and data collection parameters. $C_{40}H_{28}Co_2N_4O_4{\cdot}CHCl_3$, $M = 865.75$, crystal dimensions 0.1 × 0.1 × 0.2 mm, triclinic, space group $P\bar{1}$, $a = 11.683(3)$, $b = 12.306(3)$, $c = 15.547(4)$ Å, $\alpha = 101.84(3)$, $\beta = 101.16(3)$, $\gamma = 100.04(3)°$, $U = 2101(2)$ Å^3 (by least-squares refinement on diffractometer angles from 25 centred reflections $12 \leqslant \theta \leqslant 21°$), $T = 273(2)$ K, graphite-monochromated Mo-Kα radiation, $\lambda = 0.710\,73$ Å, $Z = 2$, $D_c = 1.321$ g cm^{-3}, $F(000) = 851.0$, μ(Mo-Kα) = 10.06 cm^{-1}.

Data were collected in the range $2 \leqslant \theta \leqslant 30°$ on an Enraf-Nonius CAD4 diffractometer using the ω–2θ scan technique. 6765 Reflections were measured, 5887 of which were assumed as observed applying the condition $I \geqslant 2.5\sigma(I)$ and used in all calculations. Three standard reflections were measured every 2 h as orientation and intensity control; significant intensity decay was not observed. Lorentz-polarization and empirical absorption corrections[33] were made (minimum and maximum corrections 0.532 and 1.298, respectively).

Structure solution and refinement. The structure was solved by direct methods, using the SHELXS 86 computer program[34] and refined on F by the full-matrix least-squares method with the SHELXL 93 computer program[35] and anisotropic thermal parameters for all non-hydrogen atoms of the dimer molecules. All H atoms (except for the $CHCl_3$ molecules) were placed in calculated positions, riding on the coordinates of the atoms to which they are attached. A weighting scheme was introduced, $w = 1/[\sigma^2(F_o^2) + (0.3195\ P)^2 + 0.17\ P]$ where $P = [\max(F_o^2) + 2F_c^2]/3$. Scattering factors were taken from ref. 36. Chlorine atoms of the first $HCCl_3$ moiety are disordered; an occupancy factor of 0.5 was assigned according to the height in the Fourier map. The second $HCCl_3$ was located with an occupancy factor of 0.5. All $HCCl_3$ groups were refined only isotropically. Final refinement converged to $R(F) = 0.047$ and $wR(F^2) = 0.1345$. Number of refined parameters was 498. Maximum shift/e.s.d. = 0.015, maximum and minimum peaks in final difference synthesis 0.93 and −0.45 e Å^{-3}, respectively (maximum around the cal atom). Calculations of geometrical parameters were made with PARST[37] and molecular graphics with ORTEP.[38]

CCDC reference number 186/701.

Results and Discussion

Ionization constants of the ligands

The ionization constants of the Schiff bases (Table 1) sal-*m*-phen, sal-2,4- and sal-2,6-toluen have been determined for the first time. For comparative purposes in Table 1 are also shown the pK_i values for the ligand 3-fluoro-*N*,*N*′-bis(salicylidene)-*o*-phenylenediamine (3-F-sal-*o*-phen).[20]

These Schiff bases are tetradentate with two adjacent weak imino donors and two strongly basic phenolate groups (Scheme 1), thus they behave as weak diprotic acids. The values obtained for the ionization constants (Table 1) are in good agreement with those reported for similar compounds such as 3-F-sal-*o*-phen[20] (Table 1) despite the differences in the solvent, ionic strength and structural features. As shown in Table 1, there is a slight increase in the pK values for sal-2,4- and sal-2,6-toluen with respect to sal-*m*-phen as a consequence of the inductive electron-donor effect of the methyl substituent on the aromatic ring.

The Schiff base *N*,*N*′-bis(salicylideneimine)ethane-1,2-diamine (H_2salen) undergoes a slow hydrolytic decomposition in strongly acid dmso–water (80:20 w/w) solution.[18] However, for sal-*m*-phen and derivatives no hydrolysis was observed above the pH range investigated (>2.5). The low basic character of *m*-phenylenediamine [log(protonation constant) = 4.31(2), this work] in dmso–water (80:20 w/w), which remains unprotonated in the media where the ethane-1,2-diamine is fully protonated,[18] is believed to be responsible for the stability of these Schiff bases and their complexes in acidic media.

The species distribution diagram as a function of $-\log[H^+]$ for sal-*m*-phen (SUP 57286) indicates that in the range pH 5–8 only the neutral Schiff base (H_2L) is present, whereas in the range pH 9–11 the species H_2L, HL^- and L^{2-} coexist. The deprotonation of both OH^- groups is completed at pH > 12.5, the only species existing being L^{2-}. Similar diagrams are obtained for sal-2,4- and sal-2,6-toluen.

Stability constants of sal-*m*-phen, sal-2,4- and sal-2,6-toluen with Cu^{II}, Ni^{II}, Co^{II} and Zn^{II}

The models that best fit the experimental potentiometric data are those that correspond to the complex species and log K values reported in Table 2.

These ligands are very versatile and can form monomers, dimers, with excess of metal and with excess of ligand species [equilibria (1)–(10)] with the metals Cu^{II}, Ni^{II}, Co^{II} and Zn^{II}, as shown in Table 2. All these species show different protonation extents. In Table 2 are also included equilibria (11) and (12). In the monomer species $[M(HL)]^+$ and [ML] the metal co-ordinates only one NO group of the ligand.[6–9] In $[MH_2L]^{2+}$ species the co-ordination of only one nitrogen can be assumed. For the dimers M_2L_2 both metals are co-ordinated to a N_2O_2 donor set from two different ligands.[14] The positive values obtained for equilibrium (12) (Table 2) indicate that the dimerization process is thermodynamically favourable as expected: in the dimers two N_2O_2 groups are involved in co-ordination with an increase in the number of chelate rings.[14] In the species with excess of ligand the metal may be four-co-ordinated by two NO groups from different ligands. Species having the ratio ligand:metal 1:2 are also obtained, in this case each metal is co-ordinated to each NO group of the Schiff base.[10]

The log K order found for the majority of species was sal-2,4-

Table 2 Stability constants of the complexes of H_2sal-*m*-phen, H_2sal-2,4- and H_2sal-2,6-toluen with Cu^{II}, Ni^{II}, Co^{II} and Zn^{II} in dmso–water (80 : 20 w/w) (25 °C, I = 0.1 mol dm^{-3} in $NaClO_4$)

	log K			
Equilibrium	Cu^{II}	Ni^{II}	Co^{II}	Zn^{II}
(*a*) sal-*m*-phen (H_2L)				
(1) $M^{2+} + H_2L \rightleftharpoons [M(H_2L)]^{2+}$	2.60(4)	2.49(2)	2.63(5)	
(2) $M^{2+} + HL^- \rightleftharpoons [M(HL)]^+$	8.13(3)	5.51(1)	5.11(3)	4.69(5)
(3) $M^{2+} + L^{2-} \rightleftharpoons [ML]$	13.02(13)	7.45(1)	7.13(6)	6.56(1)
(4) $2\,M^{2+} + HL^- + L^{2-} \rightleftharpoons [M_2(HL)L]^+$	24.40(4)	16.16(2)	15.36(5)	
(5) $2\,M^{2+} + 2\,L^{2-} \rightleftharpoons [M_2L_2]$	30.20(3)	18.04(2)	17.75(6)	16.80(1)
(6) $M^{2+} + 2\,HL^- \rightleftharpoons [M(HL)_2]$	15.40(2)	9.29(2)	8.96(4)	8.93(2)
(7) $M^{2+} + L^{2-} + HL^- \rightleftharpoons [M(HL)L]^-$		10.49(2)	10.20(5)	10.43(2)
(8) $M^{2+} + 2\,L^{2-} \rightleftharpoons [ML_2]^{2-}$		11.16(1)	11.06(3)	
(9) $2\,M^{2+} + HL^- \rightleftharpoons [M_2(HL)]^{3+}$		8.07(1)	7.64(4)	
(10) $2\,M^{2+} + L^{2-} \rightleftharpoons [M_2L]^{2+}$	16.47(2)	11.69(1)	10.82(3)	10.35(2)
(11) $[M(HL)]^+ + [ML] \rightleftharpoons [M_2(HL)L]^+$	3.25	3.20	3.12	
(12) $2\,[ML] \rightleftharpoons [M_2L_2]$	4.16	3.16	3.50	3.80
σ, χ^2	2.34, 8.4	3.4, 12.4	3.2, 11.0	2.5, 10.2
$-\log[H^+]$ range	3.4–5.3	5.0–10.2	6.2–9.6	6.3–8.5
No. titrations, no. points	6, 168	6, 303	5, 215	6, 182
(*b*) sal-2,4-toluen (H_2L)				
(1) $M^{2+} + H_2L \rightleftharpoons [M(H_2L)]^{2+}$	2.86(3)	2.50(2)	3.10(5)	2.59(3)
(2) $M^{2+} + HL^- \rightleftharpoons [M(HL)]^+$	8.32(1)	5.71(1)	5.57(3)	5.27(1)
(3) $M^{2+} + L^{2-} \rightleftharpoons [ML]$	13.42(1)	7.84(2)	7.85(5)	7.29(2)
(4) $2\,M^{2+} + HL^- + L^{2-} \rightleftharpoons [M_2(HL)L]^+$	26.03(3)	16.42(3)	16.83(5)	
(5) $2\,M^{2+} + 2\,L^{2-} \rightleftharpoons [M_2L_2]$	31.36(2)	18.67(3)	19.19(7)	18.25(4)
(6) $M^{2+} + 2\,HL^- \rightleftharpoons [M(HL)_2]$	17.65(2)	10.70(2)	10.64(6)	10.69(2)
(7) $M^{2+} + L^{2-} + HL^- \rightleftharpoons [M(HL)L]^-$		10.72(5)	11.13(5)	
(8) $M^{2+} + 2\,L^{2-} \rightleftharpoons [ML_2]^{2-}$		11.60(3)	12.12(3)	
(9) $2\,M^{2+} + HL^- \rightleftharpoons [M_2(HL)]^{3+}$		8.04(4)	8.43(3)	
(10) $2\,M^{2+} + L^{2-} \rightleftharpoons [M_2L]^{2+}$	17.20(2)	11.75(1)	11.73(3)	10.07(6)
(11) $[M(HL)]^+ + [ML] \rightleftharpoons [M_2(HL)L]^+$	4.29	2.87	3.41	
(12) $2\,[ML] \rightleftharpoons [M_2L_2]$	4.54	2.99	3.49	3.67
σ, χ^2	3.2, 12.8	3.3, 14.5	2.5, 12.1	3.2, 16.0
$-\log[H^+]$ range	3.4–5.5	5–10.3	5.6–10.1	5.7–8.1
No. titrations, no. points	6, 261	7, 352	6, 287	8, 206
(*c*) sal-2,6-toluen (H_2L)				
(1) $M^{2+} + H_2L \rightleftharpoons [M(H_2L)]^{2+}$	2.45(2)	2.36(2)	2.38(3)	
(2) $M^{2+} + HL^- \rightleftharpoons [M(HL)]^+$	8.17(1)	5.47(1)	5.01(1)	4.46(1)
(3) $M^{2+} + L^{2-} \rightleftharpoons [ML]$	12.66(1)	7.62(1)	6.90(4)	7.01(1)
(4) $2\,M^{2+} + HL^- + L^{2-} \rightleftharpoons [M_2(HL)L]^+$		15.77(4)	14.63(8)	
(5) $2\,M^{2+} + 2\,L^{2-} \rightleftharpoons [M_2L_2]$	28.14(7)	17.47(6)	16.80(5)	16.8(2)
(6) $M^{2+} + 2\,HL^- \rightleftharpoons [M(HL)_2]$	15.2(1)	10.64(1)	10.05(2)	
(7) $M^{2+} + L^{2-} + HL^- \rightleftharpoons [M(HL)L]^-$		10.51(2)	9.67(15)	10.5(1)
(8) $M^{2+} + 2\,L^{2-} \rightleftharpoons [ML_2]^{2-}$		11.10(4)	11.1(1)	
(9) $2\,M^{2+} + HL^- \rightleftharpoons [M_2(HL)]^{3+}$		8.10(2)	7.63(2)	
(10) $2\,M^{2+} + L^{2-} \rightleftharpoons [M_2L]^{2+}$	16.58(1)	11.67(1)	10.74(1)	9.83(11)
(11) $[M(HL)]^+ + [ML] \rightleftharpoons [M_2(HL)L]^+$		2.68	2.72	
(12) $2\,[ML] \rightleftharpoons [M_2L_2]$	2.87	2.23	3.00	2.80
σ, χ^2	2.8, 14.06	2.8, 16.0	2.7, 11.2	2.1, 9.6
$-\log[H^+]$ range	3.5–5.9	5.6–9.7	5.7–9.2	6.2–8.1
No. titrations, no. points	8, 248	7, 353	6, 248	4, 93

toluen > sal-*m*-phen > sal-2,6-toluen. In sal-2,4-toluen the inductive electron-donor effect of the methyl group predominates over the repulsive steric effect, contrarily for sal-2,6-toluen. The influence of the methyl substituent was found to be more important in polyaminecarboxylic acids[6–9] than in Schiff bases. The stability sequence found for most species was $Cu^{II} \gg Ni^{II} \approx Co^{II} > Zn^{II}$. The Irving–Williams order of complexation is thus fulfilled. This is consistent with the structural data for the complexes of sal-*m*-phen with Cu^{II}[14] and Co^{II} (Table 3) which indicate shorter Cu–N (1.97 Å) than Co–N (2.02 Å) bond distances.

Comparing the log K values of the stability constants of the monomer ML (Table 2) for the sal-*m*-phen ligand with those corresponding to the ML complex of the *ortho* Schiff base sal-*o*-phen[39] (with a N_2O_2 donor set) [log K(NiL) = 14.82(2), log K(CoL) = 14.64(6), log K(ZnL) = 13.31(1)], it can be seen that the log K_{ML} values for the *meta* Schiff base are practically half those corresponding to the *ortho* Schiff bases, thus indicating a donor set NO, for the former, as can be expected due to the conformation of the ligand.

The species distribution diagrams as a function of $-\log[H^+]$ show more clearly the formation of the different complex species. Fig. 1 and SUP 57286 show the diagrams for the system sal-*m*-phen–Ni^{II} in the ratio ligand : metal 1 : 1. For Co^{II} and Zn^{II} analogous diagrams are obtained. Similar diagrams are also obtained for the systems sal-2,4- and sal-2,6-toluen–M^{II} (M^{II} = Ni^{II} or Zn^{II}). For Cu^{II} the diagrams show the appearance of complex species at lower pH due to the greater values of their stability constants.

The percentage of the dimer species must increase with the concentration since equilibria (11) and (12) are displaced to the right (Table 2). At pH > 10 (pH > 7 for Cu^{II}), ML and M_2L_2 are the only species existing in the ratio 1 : 1. The diagrams also indicate that a concentrated solution with a ligand : metal ratio 1 : 1 at pH 10 is suitable for the synthesis of the dimeric complex species M_2L_2.

Table 3 Selected bond lengths (Å) and angles (°) for $[Co_2(sal\text{-}m\text{-}phen)_2]\cdot CHCl_3$ with estimated standard deviations in parentheses

Molecule 1		Molecule 2	
Co(1)–O(1)	1.912(3)	Co(2)–O(3)	1.890(4)
Co(1)–O(2)	1.917(5)	Co(2)–O(4)	1.904(5)
Co(1)–N(1)	2.008(6)	Co(2)–N(3)	2.011(6)
Co(1)–N(2)	2.027(7)	Co(2)–N(4)	2.016(3)
N(1)–Co(1)–N(2)	104.8(2)	N(3)–Co(2)–N(4)	104.0(2)
O(2)–Co(1)–N(2)	94.4(2)	O(4)–Co(2)–N(4)	94.1(2)
O(2)–Co(1)–N(1)	122.5(2)	O(4)–Co(2)–N(3)	127.4(2)
O(1)–Co(1)–N(2)	122.8(2)	O(3)–Co(2)–N(4)	123.9(2)
O(1)–Co(1)–N(1)	94.9(2)	O(3)–Co(2)–N(3)	95.2(2)
O(1)–Co(1)–O(2)	118.8(2)	O(3)–Co(2)–O(4)	114.7(2)

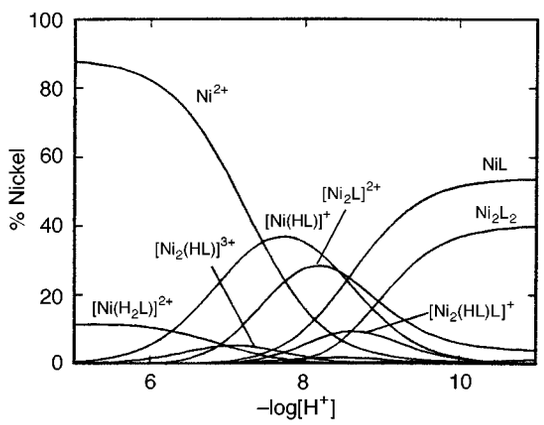

Fig. 1 Species distribution diagram as a function of $-\log[H^+]$ for the sal-*m*-phen–Ni^{II} system at ligand : metal ratio 1 : 1 and $c_M = 0.5 \times 10^{-3}$ mol dm^{-3}. Calculated from the values of log *K* given in Table 2

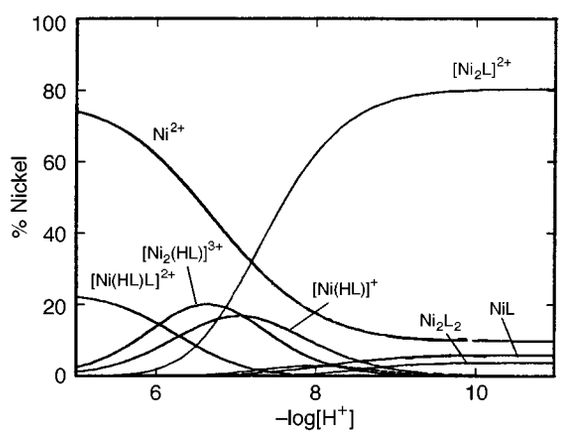

Fig. 2 Species distribution diagram as a function of $-\log[H^+]$ for the sal-*m*-phen–Ni^{II} system at ligand : metal ratio 1 : 2 and $c_M = 4 \times 10^{-3}$ mol dm^{-3}. Calculated from the log *K* values given in Table 2

In the ratio ligand : metal 2 : 1, for sal-*m*-phen–Ni^{II} (similar for Co^{II}) the species with an excess of ligand $[M(HL)_2]$, $[M(HL)L]^-$ and $[ML_2]^{2-}$ are only present at high pH. For Cu^{II} and Zn^{II} the species $[M(HL)L]^-$ and $[ML_2]^{2-}$ were not detected, due to the appearance of a precipitate at high pH (region where presumably these species should be formed).

In the ratio 1 : 2 (Fig. 2, analogous for Co^{II} and Zn^{II}) the bimetallic species is predominant at pH > 8 (>6 for Cu^{II}): both donor sites of the ligand are occupied by metal atoms.

Crystal structure

Selected bond distances and angles in the co-ordination sphere of Co^{II} are given in Table 3. The crystallographic asymmetric unit contains two half molecules (1 and 2) of $[Co_2(sal\text{-}m\text{-}phen)_2]\cdot CHCl_3$. An ORTEP drawing of molecule 1 with the atomic numbering scheme employed for all non-hydrogen atoms is shown in Fig. 3. Chloroform molecules are omitted for clarity.

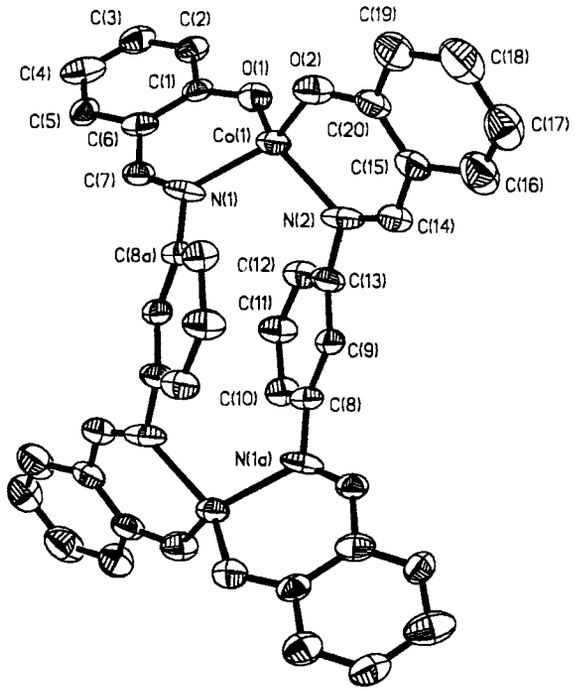

Fig. 3 An ORTEP view of the binuclear complex $[Co_2(sal\text{-}m\text{-}phen)_2]$ showing the atom labelling. Thermal ellipsoids are drawn at the 50% probability level. Hydrogen atoms and chloroform molecules are omitted for clarity. Symmetry transformation related to a: $-x + 1$, $-y$, $-z + 1$

The molecule is dimeric and centrosymmetric, with each co-ordination centre being bridged by two *m*-phenylene groups. A chloroform molecule is associated with each dimer molecule. The co-ordination about each cobalt atom can be described as distorted tetrahedral since the angle between the two salicylideneiminato-residues is 84.2(1)° and the angles N(1)–Co(1)–N(2) and N(3)–Co(2)–N(4) are 104.8(2) and 104.0(2)°, respectively, while O(2)–Co(1)–N(2) and O(4)–Co(2)–N(4) are 94.4(2) and 94.1(2)°, respectively. For the copper complex with the same ligand[14] the angles between the two salicylideneiminato-residues is 43.6°; this fact together with the bond angles around the copper atom indicates a more distorted stereochemistry for the copper than for the cobalt complex. One way to rationalize the different stereochemistry around the copper and cobalt atoms in their complexes is by using the angular overlap model, that is for sufficiently weak ligands, as in our case, the electronic configuration d^7 (Co^{II}) gives a fundamentally tetrahedral stereochemistry around the metal, while the electronic configuration d^9 (Cu^{II}) gives a stereochemistry intermediate between square planar and tetrahedral.[40]

In the cobalt complex each bridging phenylene ring makes dihedral angles of 52.8(1) and 56.7(1)° with the two chelate residues to which it is attached and are themselves parallel, the interplanar separation being 3.717(4) Å. This distance is larger than for the copper complex[14] (3.05 Å), testifying that the steric repulsion between the two bridging groups is smaller, and therefore the cobalt complex is less distorted.

The bond distances for the cobalt complex [Co–O and Co–N 1.906 and 2.016 Å (average), respectively, Table 3] are similar to those for $[Cu_2(sal\text{-}m\text{-}phen)_2]\cdot 2CHCl_3$ [Cu–O and Cu–N, respectively 1.90 and 1.97 Å (average)].[14]

Magnetic studies

The magnetic properties of copper(II), nickel(II) and cobalt(II) dinuclear complexes in the form of either χ_M the molar magnetic susceptibility per two metal ions (Ni^{II}) or $\chi_M T$ (Cu^{II} and Co^{II})

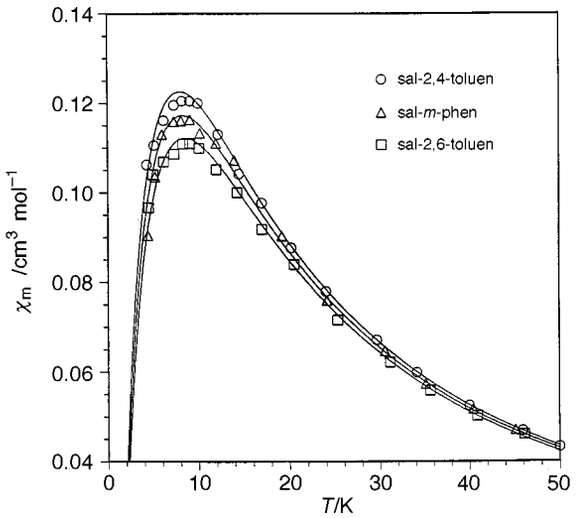

Fig. 4 Experimental molar susceptibility (per binuclear complex) for nickel(II) complexes. The solid lines represent the least-squares fit to the theoretical equation (see text)

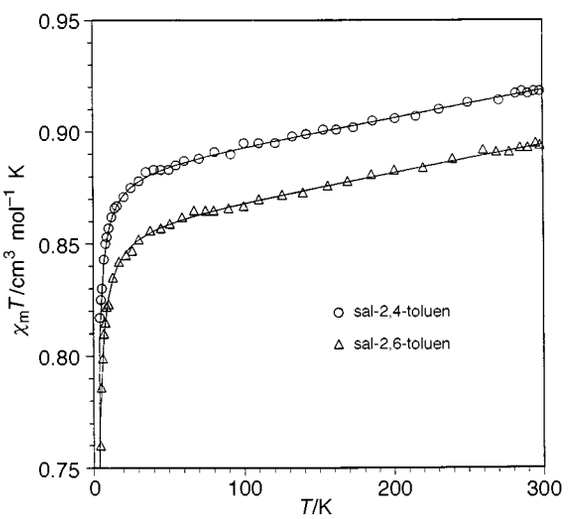

Fig. 5 Temperature dependence of $\chi_M T$ (per binuclear complex) for copper(II) complexes. Details as in Fig. 4

versus T are depicted in Figs. 4–6 and show the existence of a weak intradimer antiferromagnetic interaction. The susceptibility curves for the nickel(II) dimers have rounded maxima at *ca.* 8 K (Fig. 4) whereas no maximum of susceptibility is observed above 4.3 K for the corresponding copper(II) and cobalt(II) compounds.

The ground state of Co^{II} in a tetrahedral environment is orbitally non-degenerate, $^4A_2$, and as such it is possible to represent the intradimer magnetic interaction with the isotropic spin Hamiltonian [equation (13)]

$$H = -JS_1S_2 \qquad (13)$$

Although copper(II) and nickel(II) ions in a tetrahedral environment are orbitally degenerate ($^2T_2$ and $^3T_1$, respectively), distortions of the tetrahedral symmetry of these ions (two imino N and two phenolato O donor atoms) can cause such a significant quenching of the orbital moment of the ground state that the above spin-only formulism would be allowed. Owing to the large local zero-field splitting which is characteristic of Ni^{II} and Co^{II}, we have also considered the term $D(S_{1z^2} - S_{2z^2})$ in the Hamiltonian (13) for their dimers.[41]

Least-squares analysis of the data for dimeric complexes through the corresponding susceptibility equations derived from the above Hamiltonian leads to the parameters listed in Table 4. In the light of these values, two points deserve to be discussed: (*i*) the exchange pathway between the paramagnetic ions and (*ii*) the variation of the antiferromagnetic coupling with the nature of the metal ions.

Table 4 Exchange parameters for dimeric complexes

Ligand	Metal	$-J\,(D)$/cm^{-1}	g	$10^{-5}\,R$	$-n^2J$/cm^{-1}
sal-2,4-toluen	Cu	0.9	2.17	8.4	0.9
	Ni	2.7 (D = 1.2)	2.20	8.7	10.8
	Co	1.2	2.30	4.1	10.8
sal-*m*-phen	Cu[a]	1.0	2.16	5.1	1.0
	Ni	2.8 (D = 0.8)	2.19	5.8	11.2
		3.2 (D = 0.7)[b]	2.36[b]	—	12.8[b]
	Co	1.3	2.26	5.1	11.7
sal-2,6-toluen	Cu	1.1	2.14	6.2	1.1
	Ni	2.9 (D = 1.0)	2.18	3.1	11.6
	Co	1.4	2.23	2.0	12.6

[a] Values taken from ref. 42. [b] Values taken for the trihydrate derivative $[Ni_2(sal\text{-}m\text{-}phen)_2]\cdot 3H_2O$ from ref. 43.

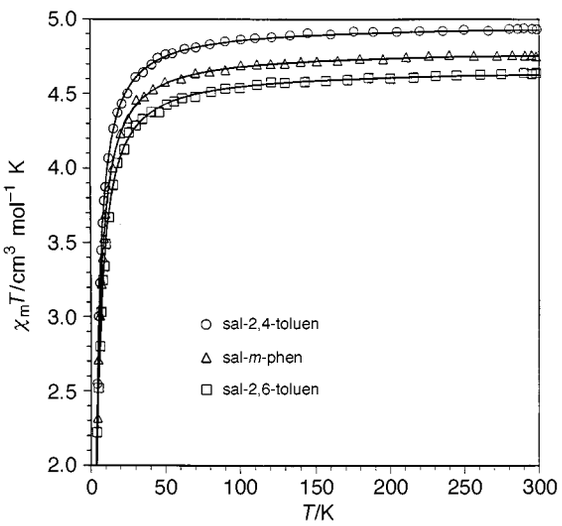

Fig. 6 Temperature dependence of $\chi_M T$ (per binuclear complex) for cobalt(II) complexes. Details as in Fig. 4

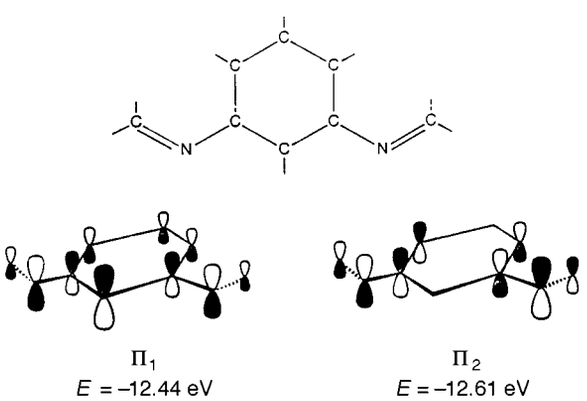

Scheme 2

Dealing with the first point, studies of magnetic exchange between paramagnetic metal ions exhibiting a tetrahedral environment are very scarce.[42,43] Tetrahedral complexes of Cu^{II}, Ni^{II} and Co^{II} present magnetic orbitals of t_2 symmetry and, as such, the π interaction with the ligands can be very important. In addition, it has been suggested that the magnetic interaction through extended bridging ligands having a π-conjugated system is mediated *via* the delocalized π framework.[44] In fact, extended Hückel calculations§[45] on the *m*-phenylenediimine

§ The atomic parameters in the Hückel calculations were taken from ref. 46.

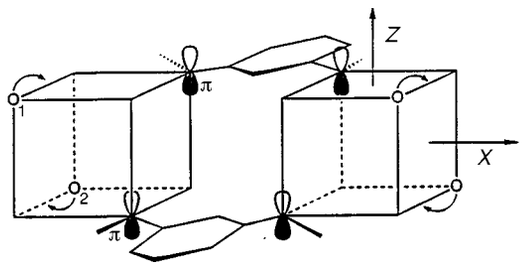

Scheme 3

bridging fragment (see Scheme 2) show that the two highest occupied molecular orbitals (HOMOs) are of π symmetry (π_1 and π_2 in Scheme 2). So, assuming that the magnetic interaction in these dimeric compounds is mediated *via* the π_1 and π_2 HOMOs from the delocalized π system of the *m*-phenylenediimine bridging fragment and taking into account the structure of these complexes, Scheme 3 can be used to describe the magnetic interaction therein. One can see that the overlap between the $3d_{xy}$ type magnetic orbital of the metal ion and the p orbital of the bridging ligand is greater than that involving the $3d_{xz}$ and $3d_{yz}$, whereas the overlap with the phenolato-oxygens (p_x, p_y and p_z) is identical for the three 3d orbitals. In this respect, the trend of the orbital energy will be $\varepsilon_{d_{xy}} > \varepsilon_{d_{xz}} \approx \varepsilon_{d_{yz}}$ and due to the larger overlap between the d_{xy} orbital and the bridging ligand this $3d_{xy}$ orbital will be mainly responsible for the magnetic interaction[47] in the complexes of Ni^{II} and Co^{II} which exhibit the electronic configurations $(d_{z^2})^2(d_{x^2-y^2})^2(d_{xz},\ d_{yz})^3(d_{xy})^1$ and $(d_{z^2})^2(d_{x^2-y^2})^2(d_{xz},\ d_{yz})^2(d_{xy})^1$. Looking at the copper(II) complexes, a distortion of the tetrahedron occurs, consisting of a shift of the phenolato oxygens in such a way that they are occupying the middle point of the edge as shown in Scheme 3. Consequently, the angle between the O(1)···O(2) and N(1)···N(2) vectors is 45°,[14] in contrast to the value of *ca.* 90° observed in the case of the cobalt(II) complexes and which we assume to be the same for the nickel(II) series. Such a distortion in the copper(II) family causes a larger interaction between the d_{xz} orbital and the phenolato oxygens, and raises the energy of this orbital placing it above that of d_{xy}. However, this distortion does not modify significantly the overlap between the d_{xz} orbital and the bridging ligand. So, the electronic configuration for the copper(II) complexes exhibiting the above-mentioned distortion is $(d_{z^2})^2(d_{x^2-y^2})^2(d_{yz})^2(d_{xy})^2(d_{xz})^1$. The magnetic orbital in this case, d_{xz}, interacts poorly with the bridge, leading to a weaker magnetic coupling than in the related complexes of Ni^{II} and Co^{II} where the magnetic orbital is of the d_{xy} type.

These simple considerations allow us to analyse the second key point, that is the variation of the value of *J* as a function of the metal ion for a given ligand. In order to do this one must take into account that when the metal ions have more than one unpaired electron the experimental *J* parameter can be decomposed into a sum of individual contributions, $J_{\mu\nu}$, from each pair of magnetic orbitals involved in the exchange phenomenon [equation (14)],[48] where n_A and n_B are the numbers

$$J = \frac{1}{n_A n_B} \sum_{\mu=1}^{n_A} \sum_{\nu=1}^{n_B} J_{\mu\nu} \qquad (14)$$

of unpaired electrons on the metal ions A and B. In our case $n_A = n_B = n = 1$ (Cu^{II}), 2(Ni^{II}) and 3(Co^{II}). This equation shows how the magnitude of the net antiferromagnetic interaction is not properly described by *J* but by n^2J, which has also been included in Table 4. From equation (2) and neglecting the ferromagnetic terms $J_{\mu\nu}$ (with $\mu = \nu$) (it is well known that the more extended the bridge the weaker are the ferromagnetic terms)[49] we have equations (15)–(17). Given that (see above)

$$J_{CoCo} \approx \tfrac{1}{9}(J_{xy,xy} + J_{xz,xz} + J_{yz,yz}) = -1.3\ cm^{-1} \qquad (15)$$

$$J_{NiNi} \approx \tfrac{1}{4}[J_{xy,xy} + \tfrac{1}{2}(J_{xz,xz} + J_{yz,yz})] = -2.9\ cm^{-1} \qquad (16)$$

$$J_{CuCu} = J_{xz,xz} = -1\ cm^{-1} \qquad (17)$$

$J_{xy,xy} \gg J_{xz,xz} \gg J_{yz,yz}$, equations (18)–(20) are obtained from (15)–(17), the agreement between the theoretical and experimental data being satisfactory.

$$9J_{CoCo} \approx J_{xy,xy} \approx -11.7\ cm^{-1} \qquad (18)$$

$$4J_{NiNi} \approx J_{xy,xy} \approx -11.6\ cm^{-1} \qquad (19)$$

$$J_{CuCu} \approx J_{xz,xz} \approx -1\ cm^{-1} \qquad (20)$$

This result strongly suggests that the antiferromagnetic interaction in these dimers must be mediated *via* the delocalized π framework of the *m*-phenylenediimine fragment.

Acknowledgements

Financial support from the Dirección General de Investigación Científica y Técnica (DGICYT) (Spain) through Project PB89-0401 and Action APC 94-0031, the Spanish–Italian Integrated Actions 1993 HI 123A, and the Human Capital and Mobility Program (Network on Metals and Environmental Problems, E. C.) through grant ERBCHRX-CT94-0632 is gratefully acknowledged.

References

1 N. Nakasuka, M. Kunimatsu, K. Matsumura and M. Tanaka, *Inorg. Chem.*, 1985, **24**, 10.
2 F. Brito, A. Mederos, J. V. Herrera, S. Domínguez and M. Hernández-Padilla, *Polyhedron*, 1988, **7**, 1187.
3 E. F. K. McCandlish, T. K. Michael, J. A. Neal, E. C. Lingafelter and N. J. Rose, *Inorg. Chem.*, 1978, **17**, 1383.
4 N. Nakasuka, Sh. Azuma and M. Tanaka, *Acta Crystallogr.*, *Sect. C*, 1986, **42**, 673.
5 M. Hernández-Padilla, S. Domínguez, P. Gili, A. Mederos and C. Ruíz-Pérez, *Polyhedron*, 1992, **11**, 1965.
6 M. Hernández-Padilla, J. Sanchiz, S. Domínguez, A. Mederos, J. M. Arrieta and F. J. Zúñiga, *Acta Crystallogr.*, *Sect. C*, 1996, **52**, 1618.
7 A. Mederos, P. Gili, S. Domínguez, A. Benítez, M. S. Palacios, M. Hernández-Padilla, P. Martín-Zarza, M. L. Rodríguez, C. Ruiz-Pérez, F. G. Lahoz, L. A. Oro, F. Brito, J. M. Arrieta, M. Vlassi and G. Germain, *J. Chem. Soc.*, *Dalton Trans.*, 1990, 1477.
8 S. Domínguez, A. Mederos, P. Gili, A. Rancel, A. E. Rivero, F. Brito, F. Lloret, X. Solans, C. Ruiz-Pérez, M. L. Rodríguez and I. Brito, *Inorg. Chim. Acta*, 1997, **255**, 367.
9 S. Domínguez, A. Rancel, V. Herrera, A. Mederos and F. Brito, *J. Coord. Chem.*, 1992, **25**, 271.
10 C. Ruiz-Pérez, M. L. Rodríguez, F. V. Rodríguez-Romero, A. Mederos, P. Gili and P. Martín-Zarza, *Acta Crystallogr.*, *Sect. C*, 1990, **46**, 1405.
11 C. A. González, M. Hernández-Padilla, S. Domínguez, A. Moderos, F. Brito and J. M. Arrieta, *Polyhedron*, 1997, **16**, 2925.
12 N. B. Pahor, M. Calligaris, P. Delise, G. Dodic, G. Nardin and L. Randaccio, *J. Chem. Soc.*, *Dalton Trans.*, 1976, 2478.
13 R. Hernández-Molina, A. Mederos, P. Gili, S. Domínguez, P. Núñez, G. Germain and T. Debaerdemaeker, *Inorg. Chim. Acta*, 1997, **256**, 319.
14 C. A. Bear, J. M. Waters and T. N. Waters, *J. Chem. Soc. A*, 1970, 2494.
15 A. Mederos, F. G. Manrique, A. Medina and G. de la Fuente, *An. Quim. B*, 1983, **79**, 377.
16 F. Lloret, M. Mollar, J. Faus, M. Julve and W. Díaz, *Inorg. Chim. Acta*, 1991, **189**, 195.
17 F. Lloret, J. Moratal and J. Faus, *J. Chem. Soc.*, *Dalton Trans.*, 1983, 1743.
18 F. Lloret, J. Moratal and J. Faus, *J. Chem. Soc.*, *Dalton Trans.*, 1983, 1749.
19 F. Lloret, M. Mollar, J. Moratal and J. Faus, *Inorg. Chim. Acta*, 1986, **124**, 67.
20 R. A. Motekaitis and A. E. Martell, *Inorg. Chem.*, 1988, **27**, 2718.

21 A. Mederos, F. G. Manrique and A. Medina, *An. Quim. B*, 1980, **76**, 33.
22 G. Schwarzenbach and M. Flaschka, *Complexometric Titrations*, Methuen, London, 1957.
23 E. Chinea, S. Domínguez, A. Mederos, F. Brito, J. M. Arrieta, A. Sánchez and G. Germain, *Inorg. Chem.*, 1995, **34**, 1579.
24 M. Fontanelli and M. A. Michelona, Spanish–Italian Congress on Thermodynamics of Metal Complexes, Peñíscola, Sevicio de Publicaciones, Diputación de Castellón, 1990, p. 41.
25 G. Biederman and L. G. Sillén, *Ark. Kemi*, 1953, **5**, 425.
26 P. Gans, A. Sabatini and A. Vacca, *J. Chem. Soc.*, *Dalton Trans.*, 1985, 1195.
27 A. Earnshaw, *Introduction to Magnetochemistry*, Academic Press, London and New York, 1968.
28 A. Mederos, F. G. Manrique and A. Medina, *An. Quim. B*, 1980, **76**, 37.
29 A.B. P. Lever, *Inorganic Electronic Spectroscopy*, 2nd edn., Elsevier, Amsterdam, 1984, pp. 496–500.
30 P. Gili, P. Martín-Zarza, P. Núñez, A. Medina, M. C. Díaz, M. G. Martín, J. M. Arrieta, M. Vlassi, G. Germain, M. Vermeire and L. Dupont, *J. Coord. Chem.*, 1989, **20**, 273.
31 A. Castiñeiras, J. A. Castro, M. L. Durán, J. A. García-Vázquez, A. Macias, J. Romero and A. Sousa, *Polyhedron*, 1989, **8**, 2549.
32 E. Labisbal, J. A. García-Vázquez, J. Romero, S. Picos, A. Sousa, A. Castiñeiras and C. Maichle-Mössmer, *Polyhedron*, 1995, **14**, 663.
33 DIFABS, N. Walker and D. Stuart, *Acta Crystallogr.*, *Sect. A*, 1983, **39**, 158.
34 SHELXS 86, G. M. Sheldrick, *Acta Crystallogr.*, *Sect. A*, 1990, **46**, 467.
35 G. M. Sheldrick, SHELXL 93, Program for the Refinement of Crystal Structures, University of Göttingen, 1993.
36 *International Tables for X-Ray Crystallography*, Kynoch Press, Birmingham, 1974, vol. 4, pp. 99 and 149.
37 M. Nardelli, PARST, *Comput. Chem.*, 1983, **7**, 95.
38 C. K. Johnson, ORTEP, Report ORNL-3794, Oak Ridge National Laboratory, Oak Ridge, TN, 1971.
39 R. Hernández-Molina, A. Mederos, P. Gili, S. Domínguez and P. Núñez, *Polyhedron*, in the press.
40 K. F. Purcell and J. C. Kotz, *Inorganic Chemistry*, W. B. Saunders Co., Philadelphia, 1977, p. 543.
41 G. De Munno, M. Julve, F. Lloret and A. Derory, *J. Chem. Soc.*, *Dalton Trans.*, 1993, 1179; A. P. Ginsberg, R. L. Martin, R. W. Brookes and R. C. Sherwood, *Inorg. Chem.*, 1972, **11**, 2884.
42 D. Y. Jeter and W. E. Hatfield, *Inorg. Chim. Acta*, 1972, **6**, 440.
43 E. F. Hasty, L. J. Wilson and D. N. Hendrickson, *Inorg. Chem.*, 1978, **17**, 1834.
44 A. M. W. C. Thompson, D. Gatteschi, J. A. McCleverty, J. A. Navas, E. Rentschler and M. D. Ward, *Inorg. Chem.*, 1996, **25**, 2701; A. Wlodarczyk, J. P. Maher, J. A. McCleverty and M. D. Ward, *J. Chem. Soc.*, *Chem. Commun.*, 1995, 2397.
45 C. Mealli and D. M. Proserpio, Computer Aided Composition of Atomic Orbitals (CACAO) Program, PC Version, 1992; see *J. Chem. Educ.*, 1990, **67**, 339.
46 S. Alvarez, M. Julve and M. Verdaguer, *Inorg. Chem.*, 1994, **29**, 4501.
47 J. J. Girerd, M. F. Charlot and O. Khan, *Mol. Phys.*, 1997, **34**, 1603; O. Khan and M. F. Charlot, *Nouv. J. Chim.*, 1980, **4**, 567.
48 O. Kahn, *Struct. Bonding* (*Berlin*), 1987, **68**, 89.
49 O. Kahn, *Comments Inorg. Chem.*, 1984, **3**, 105.

Received 1*st April* 1997; *Paper* 7/02151H